



Published in final edited form as:

*Circulation*. 2012 June 5; 125(22): 2698–2706. doi:10.1161/CIRCULATIONAHA.112.094714.

## Ranolazine Decreases Mechanosensitivity of the Voltage-Gated Sodium Ion Channel $Na_V1.5$ : A Novel Mechanism of Drug Action

Arthur Beyder, MD, PhD<sup>1</sup>, Peter R. Strege, MS<sup>1</sup>, Santiago Reyes, PhD<sup>2</sup>, Cheryl E. Bernard, MS<sup>1</sup>, Andre Terzic, MD, PhD<sup>2</sup>, Jonathan Makielski, MD<sup>3</sup>, Michael J. Ackerman, MD, PhD<sup>2</sup>, and Gianrico Farrugia, MD<sup>1</sup>

<sup>1</sup>Division of Gastroenterology & Hepatology, Enteric Neuroscience Program, Rochester, MN

<sup>2</sup>Division of Cardiovascular Diseases, Dept of Medicine, Mayo Clinic, Rochester, MN

<sup>3</sup>Dept of Medicine, Division of Cardiovascular Medicine, University of Wisconsin, Madison, WI

### Abstract

**Background**— $Na_V1.5$  is a mechanosensitive voltage gated sodium-selective ion channel responsible for the depolarizing current and maintenance of the action potential plateau in the heart. Ranolazine is a  $Na_V1.5$  antagonist with anti-anginal and anti-arrhythmic properties.

**Methods and Results**—Mechanosensitivity of  $Na_V1.5$  was tested in voltage-clamped whole cells and cell-attached patches by bath flow and patch pressure, respectively. In whole cells, bath flow increased peak inward current in both murine ventricular cardiac myocytes ( $24 \pm 8\%$ ) and HEK cells heterologously expressing  $Na_V1.5$  ( $18 \pm 3\%$ ). The flow-induced increases in peak current were blocked by ranolazine. In cell-attached patches from cardiac myocytes and  $Na_V1.5$ -expressing HEK cells, negative pressure increased  $Na_V$  peak currents by  $27 \pm 18\%$  and  $18 \pm 4\%$  and hyperpolarized voltage dependence of activation by  $-11$  mV and  $-10$  mV, respectively. In HEK cells, negative pressure also increased the window current (250%) and increased late open channel events (250%). Ranolazine decreased pressure-induced shift in the voltage-dependence ( $IC_{50}$  54  $\mu$ M) and eliminated the pressure-induced increases in window current and late current event numbers. Block of  $Na_V1.5$  mechanosensitivity by ranolazine was not due to the known binding site on DIVS6 (F1760). The effect of ranolazine on mechanosensitivity of  $Na_V1.5$  was approximated by lidocaine. However, ionized ranolazine and charged lidocaine analog (QX-314) failed to block mechanosensitivity.

**Conclusions**—Ranolazine effectively inhibits mechanosensitivity of  $Na_V1.5$ . The block of  $Na_V1.5$  mechanosensitivity by ranolazine does not utilize the established binding site, and may require bilayer partitioning. Ranolazine block of  $Na_V1.5$  mechanosensitivity may be relevant in disorders of mechano-electric dysfunction.

### Keywords

drugs; electrophysiology; ion channels; mechanics; myocytes

---

**Correspondence:** Gianrico Farrugia, MD Division of Gastroenterology & Hepatology Enteric Neuroscience Program Mayo Clinic 200 First Street SW Rochester, MN 55905 Tel: 507-284-1911 Fax: 507-284-0266 farrugia.gianrico@mayo.edu.

**Conflict of Interest Disclosures:** None.

**Publisher's Disclaimer:** This is a PDF file of an unedited manuscript that has been accepted for publication. As a service to our customers we are providing this early version of the manuscript. The manuscript will undergo copyediting, typesetting, and review of the resulting proof before it is published in its final citable form. Please note that during the production process errors may be discovered which could affect the content, and all legal disclaimers that apply to the journal pertain.

## Introduction

Electro-mechanical coupling in the cardiac myocyte is vital for the generation of contraction. In turn, mechano-electric feedback (MEF) has an important regulatory role. Physiologic roles of MEF include stretch-related changes in sinoatrial node pacing frequency<sup>1</sup>, ventricular and atrial excitability<sup>2</sup> and conduction velocity<sup>3</sup>. Acute mechano-electric dysfunction is a known pathophysiologic mechanism<sup>4</sup>, yet commonly, MEF pathologies are caused by chronic abnormalities of preload and afterload leading to stretch-related electrical disturbances<sup>5</sup>.

Redundancy in biological tissues exists to regulate MEF at cellular and molecular levels. Membrane tension opens stretch-activated channels (SACs), thus modulating electrical excitability<sup>6</sup>. However, molecular identities of mammalian non-selective cation stretch-activated channels remain elusive. Voltage-gated ion channels are also mechanically sensitive<sup>7</sup>. They are attractive MEF targets due to high density of expression and direct involvement in the coordination of electrical activity. Na<sub>v</sub>1.5 is the principal voltage-gated sodium channel in cardiac myocytes<sup>8</sup>. Na<sub>v</sub>1.5 is mechanosensitive and classic SACs blockers are known to inhibit this channel<sup>9, 10</sup>. Acute stretch shifts Na<sub>v</sub>1.5 voltage dependence of activation and inactivation<sup>11</sup>, resulting in accelerated kinetics<sup>11, 12</sup>, increased peak currents<sup>13</sup> and stabilization of inactivation<sup>11</sup>. The piperazine-derivative ranolazine is a Na<sub>v</sub>1.5 antagonist and an anti-anginal with anti-arrhythmic properties<sup>14</sup> that shows promise for management of heart failure<sup>15</sup>. The molecular mechanism of ranolazine for ischemia could be through block of persistent (i.e., late) Na<sub>v</sub>1.5 current<sup>16</sup>. Effects of ranolazine may also result from its hyperpolarizing shift in voltage-dependence of steady-state inactivation similar to the inactivated-state blocker lidocaine<sup>14</sup>. The function of lipid soluble drugs such as lidocaine<sup>17</sup> and ranolazine may rely on partitioning into the lipid bilayer<sup>18</sup>. Na<sub>v</sub> channels are modulated by the cytoskeleton<sup>19</sup> & amphipaths<sup>20</sup>, and the biochemical and mechanical states of the lipid bilayer<sup>21</sup> impact mechanosensitivity of voltage-gated ion channels.

We hypothesized that ranolazine may modulate the mechanical behavior of Na<sub>v</sub>1.5. Our results show that the Na<sub>v</sub> channels native to cardiac myocytes or Na<sub>v</sub>1.5 transfected in HEK are mechanically sensitive. Ranolazine effectively blocks Na<sub>v</sub> and Na<sub>v</sub>1.5 mechanosensitivity, possibly via bilayer partitioning. Its mechanism is not due to binding to its established binding site.

## Methods

### Adult Murine Cardiac Myocyte Dissociation

Nine to eleven week old BALB/c mice (Harlan Sprague-Dawley, Indianapolis, IN) were used for the isolation of the ventricular cardiac myocytes as previously described<sup>22</sup> and detailed in Supplementary Methods. The mice were maintained and the experiments were performed with approval from the Institutional Animal Care and Use Committee of the Mayo Clinic.

**Cell culture**—Human embryonic kidney 293 (HEK) cells were cultured and transfected as previously described<sup>11</sup> (**Supplemental Methods**).

### Recording solutions & Pharmacology

Recording solutions are detailed in Supplementary Methods. Ranolazine and lidocaine were diluted in bath or patch solution from 10 mM ethanol stocks. QX-314 was prepared daily from powder at 500 μM working concentration in pipette solution.

## Electrophysiology

Electrodes were pulled using Sutter Instruments P-97 puller and coated with heat cured Dow Corning R6101 compound from Kimble KG-12 and Garner 8250 glass for whole-cell and patch experiments, respectively. Axon 200A amplifier, Digidata 1322A, and Clampex 9 software were used for voltage-clamp and data acquisition.

### Whole cell electrophysiology

A single 18 sweep, 90 sec pulse protocol was designed to measure peak current, voltage dependence, and kinetics of activation and inactivation. Cells were held at -120 mV, stepped to test pulses from -130 mV to 30 mV at 5 or 10 mV intervals for 3 sec, then to -120 mV for 0.1 msec, then to a second test pulse at -30 mV for 100 msec. The sampling rate was 20 kHz and intersweep interval was 5 sec.

### Cell-attached patches

Electrodes were fire polished specifically for patch mechano-activation as previously published<sup>11</sup>. Seals were observed for 5 minutes for stabilization. For voltage-ladder protocols, a 1 Hz stimulation frequency was used with a P/4 protocol and no interpulse delay. Cells were held at -100 mV, and at each step a 4 msec pre-pulse to -204 mV accelerated recovery from inactivation before stepping in 10 mV increments from -140 mV to 10 mV for 80 msec per step to test activation and finally a step to 0 mV for 10 msec to test availability. A 10x average was obtained for each voltage step.

For single channel experiments, currents were digitized at 10 kHz and filtered at 2 kHz using a low-pass Bessel filter. Window protocol was a sequence of 300 msec long pulses at a specific HP, determined to be at the foot of the IV curve. Pressure was applied for 100 msec in the middle of each pulse. Late current protocol was a train of depolarizations from HP -100 mV to 0 mV for 200 msec with a 1.1 sec interpulse interval.

### Mechanical stimulation

Mechanical stimuli consisted of flow and patch pressure for whole cell and cell-attached patches, respectively. Flow of solution through a 0.7 mL elliptical bath chamber was calibrated at 10 mL/min. Specialized rapid pressure clamp was used to apply pressure (courtesy of Dr. Fred Sachs' lab)<sup>23</sup>. Negative pressure produced patch stretch by displacement (**Supplemental Movie 1**) and was closely monitored during patch formation and pressure delivery for each of the protocols<sup>24</sup>. Length of mechanical stimuli was <100 msec to minimize structural remodeling (**Supplemental Methods**).

### Data Analysis

Whole cell and macroscopic patch data were analyzed in Pclamp 9 while single channel data were analyzed in QUB (www.qub.buffalo.edu). Voltage dependence and dose-response curves were fit in pClamp9 and Origin 8.61 (**Supplemental Methods**). For whole cell experiments significance was assigned when  $P < 0.05$  by a two-way repeated measures ANOVA with Bonferroni multiple comparisons posttest in GraphPad Prism 5 (**Figure 1**, **Figure 6**). For experiments on patches significance was  $P < 0.05$  by Student's t-tests as specified in the text, and specifically two-tailed paired t-tests (**Figure 4**, **Figure 5**) and two-tailed two-sample equal variance t-tests (**Figure 7**, **Figure 8**) in Origin 8.61.

## Results

### Ranolazine inhibits the flow-induced increase in peak current in murine cardiomyocytes

We used a 10 mL/min bath flow to simulate shear stress of voltage clamped murine cardiac ventricular myocytes in a control solution and then in the presence of 50  $\mu$ M ranolazine. Flow of the control solution increased peak  $\text{Na}^+$  current from  $-28.0 \pm 4.7$  pA/pF to  $-35.9 \pm 8.2$  pA/pF, or by  $24 \pm 8\%$  ( $n=5$ ,  $P < 0.05$ , **Figure 1A**). In the same cells, 50  $\mu$ M ranolazine decreased peak  $\text{Na}^+$  current from  $-28.0 \pm 4.7$  pA/pF to  $-9.3 \pm 1.7$  pA/pF, or by  $68 \pm 3\%$  ( $n=5$ ,  $P < 0.05$ ). Ranolazine also blocked the flow-induced increase of peak  $\text{Na}^+$  current from  $-9.3 \pm 1.7$  pA/pF with ranolazine to  $-10.2 \pm 2.4$  pA with ranolazine and bath flow, ( $6 \pm 7\%$ ,  $n=5$ ,  $P > 0.05$ , **Figure 1A**). These data show that in cardiac myocytes ranolazine not only blocks peak  $\text{Na}_V$  current but also inhibits the response of  $\text{Na}_V$  channels to mechanical stimulation by bath flow.

### Ranolazine decreases $\text{Na}_V1.5$ peak current at rest and abolishes increase in current in response to bath flow in HEK cells

$\text{Na}_V1.5$  is the predominant voltage-gated sodium channel in the adult murine<sup>25</sup> and human<sup>8</sup> cardiac myocytes. Next, we examined HEK cells heterologously expressing  $\text{Na}_V1.5$   $\alpha$ -subunit. Mechanical stimulation by flow increased  $\text{Na}_V1.5$  maximum peak  $\text{Na}^+$  current from  $-137 \pm 16$  pA/pF for control to  $-161 \pm 19$  pA/pF for flow, or by  $18 \pm 3\%$  ( $n=9$ ,  $P < 0.05$ , **Figure 1B**). Bath flow also accelerated the time constants of activation from  $0.67 \pm 0.06$  msec to  $0.49 \pm 0.05$  msec and inactivation from  $0.87 \pm 0.08$  msec to  $0.77 \pm 0.07$  msec ( $n=8$ ,  $P < 0.05$ , **Supplementary Figure 1A**), consistent with published data<sup>26</sup>. Subsequent 10 min exposure to 50  $\mu$ M ranolazine reduced maximum peak  $\text{Na}^+$  current from  $-137 \pm 16$  pA/pF to  $-90 \pm 13$  pA/pF, or by  $37 \pm 5\%$  ( $n=9$ ,  $P < 0.05$ ) and inhibited the response to flow from  $-90 \pm 13$  pA/pF with ranolazine to  $-100 \pm 14$  pA/pF with ranolazine and bath flow, ( $10 \pm 3\%$ ,  $n=9$ ,  $P > 0.05$ ). Block by ranolazine significantly interacted with mechanical activation of  $\text{Na}_V1.5$ , whereas the measurement of all other parameters such as voltage dependence and kinetics revealed no effect ( $P < 0.05$  interaction for peak current, **Figure 1B**); and  $P > 0.05$  for voltage dependence or kinetics, **Supplemental Figure 1A**). These data suggest that ranolazine can block current at rest and inhibit the mechanical activation of  $\text{Na}_V1.5$  expressed in HEK cells similar to  $\text{Na}_V$  channels in cardiac myocytes.

### Ranolazine reduces pressure-induced hyperpolarizing shift in the voltage sensitivity of $\text{Na}_V1.5$

To address the possibility that the effect of ranolazine could be dependent on the stimulus, we also tested the effect of ranolazine on  $\text{Na}_V1.5$  mechanosensitivity by pressure clamp on cell patches. Since ranolazine partitions readily into cell membranes (partition coefficient 1.53<sup>18</sup>) we were able to add the drug to the bath solution with rapid effect (time constant  $\tau = 19.4 \pm 1.6$  sec, **Supplemental Figure 2**). In  $\text{Na}_V1.5$  expressing HEK cells, addition of 50  $\mu$ M ranolazine decreased peak currents by  $-32 \pm 8\%$  ( $n=4$ ,  $P < 0.05$ , paired t-test), similar to the HEK whole-cell results above.

Before the application of ranolazine, the average peak patch current in the transfected cells was  $-78.6 \pm 69.2$  pA ( $n=7$ ). A  $-30$  mmHg 100 msec long pressure pulse was applied at each voltage step during the subsequent ladder protocol of 17 steps from  $-140$  to  $30$  mV by  $10$  mV increments. Patch pressure produced an increase in current amplitude of  $+18 \pm 4\%$  ( $n=7$ ,  $P < 0.05$ , paired t-test) and accelerated kinetics at all steps as shown for  $-100$  mV (dash dot),  $-50$  mV (dot) and  $-30$  mV (solid) (**Figure 2A**). Since pressure accelerated the kinetics of both activation and inactivation and increased peak currents, there was a significant difference current ( $I_{30} - I_0$ ) (**Figure 2B**). For depolarization at the foot of the activation curve, pressure produced a significant increase in inward current, and a large inward difference

current (dotted trace). For the large depolarization that is fully activating, the difference current was biphasic, with large early inward difference current followed by significantly decreased inward flux later in the pulse (solid trace).

In **Figure 2C** peak currents from step 1 and step 2 from a typical patch are plotted against voltage, showing voltage dependence of activation (squares) and availability (circles) at rest (0 mmHg) (black) and with -30 mmHg pressure (grey). Solid lines are Boltzmann fits of the peaks at the indicated voltages (solid lines). On average, for a -30 mmHg stimulus, shift in the voltage dependence of activation ( $\Delta V_{1/2a}$ ) was  $-10.1 \pm 1.5$  mV ( $n=7$ ,  $P<0.05$ , paired t-test) and shift in the voltage dependence of inactivation ( $\Delta V_{1/2i}$ ) was  $-12.1 \pm 1.7$  mV ( $n=6$ ,  $P<0.05$ , paired t-test), peak  $\text{Na}^+$  current change ( $\Delta I_{\text{peak}}$ ) was  $18 \pm 4\%$  ( $n=7$ ,  $P<0.05$ , paired t-test). We found no significant change in slopes ( $\Delta dV_a = 0.1 \pm 0.3$  mV,  $\Delta dV_i = 2.9 \pm 3.2$  mV,  $P>0.05$  for both). These data demonstrate an increase in peak current, a shift in the voltage dependency of  $\text{Na}_v1.5$  current with pressure, suggesting that the channels will activate at more hyperpolarized voltages, which would make a cardiac myocyte more excitable.

After the addition of 50  $\mu\text{M}$  ranolazine a -30 mmHg pressure failed to increase peak current and accelerate kinetics as for the control above, as exemplified in the raw traces (**Figure 2D**) and lack of difference current (**Figure 2E**). In the presence of 50  $\mu\text{M}$  ranolazine, the half-point of the voltage dependence of activation ( $V_{1/2a}$ ) did not shift with pressure (black is 0 mmHg, grey is -30 mmHg). Pressure resulted in an average  $\Delta V_{1/2a}$  of  $-6.4 \pm 0.7$  mV, which is smaller than with 0  $\mu\text{M}$  ranolazine ( $n=5$ ,  $P<0.05$ , two sample t-test) (**Figure 2F**). The peak current change ( $\Delta I_{\text{peak}} = 14 \pm 4\%$ ) and shift in the voltage dependence of steady state inactivation ( $\Delta V_{1/2i} = -8.7 \pm 0.5$  mV) with pressure were not statistically different from 0  $\mu\text{M}$  ranolazine, ( $n=5$ ,  $P>0.05$  compared with 0  $\mu\text{M}$  ranolazine, two-sample t-test). Also, no significant change was found for slope change ( $\Delta dV_a = 0.11 \pm 0.29$  mV,  $\Delta dV_i = 2.93 \pm 3.23$  mV,  $P>0.05$ , two-sample t-test).

We determined the potency of ranolazine inhibition of  $\text{Na}_v1.5$  mechanosensitivity. The voltage-dependence of activation ( $V_{1/2a}$ ) and steady-state inactivation ( $V_{1/2i}$ ) half-points from Boltzmann fits of IV curves for patches at rest (0 mmHg) and pressure (-30 mmHg) were obtained in the absence and presence of ranolazine at concentrations of 10, 50, 100, 300  $\mu\text{M}$  ( $n = 3$  per concentration). Pressure-dependence of the shift in the voltage-dependence of activation ( $\Delta V_{1/2a}$ ) was fit to a dose-response curve with an  $\text{IC}_{50}$  of 53.6  $\mu\text{M}$  and hill slope  $h = -0.01$  (**Figure 3**). Ranolazine also affected the mechanosensitivity of the voltage dependence of inactivation ( $\Delta V_{1/2i}$ ) and peak current ( $I_{30}/I_0$ ), but these effects were more difficult to quantify since ranolazine is known to affect both of these parameters at rest<sup>14</sup> (**Supplemental Figure 4**). Thus, we elected to use  $\Delta V_{1/2a}$  as an assay for pressure-effects of ranolazine on  $\text{Na}_v1.5$ .

We next examined  $\text{Na}_v$  pressure sensitivity and the ranolazine effect in a native system, using cell-attached patches in murine myocytes. In cell-attached patches from adult murine ventricular cardiac myocytes voltage dependent inward  $\text{Na}^+$  current peaked at  $-184 \pm 223$  pA and increased to  $-263 \pm 372$  pA in response to -20 mmHg patch pressure, or by  $27 \pm 18\%$  ( $n=5$ ,  $P<0.05$ , paired t-test). Patch pressure hyperpolarized the voltage-dependence of activation, shifting  $V_{1/2a}$  by  $-11.4 \pm 6.7$  mV ( $n=5$ ,  $P<0.05$ , paired t-test). Addition of 50  $\mu\text{M}$  ranolazine decreased peak currents to  $-65 \pm 35$  pA, or by 65% percent compared to no ranolazine controls ( $n=6$ ,  $P<0.05$ , two-sample t-test). In the presence of 50  $\mu\text{M}$  ranolazine negative pressure (-20 mmHg) produced a 66% smaller hyperpolarizing shift in the voltage-dependence of activation  $V_{1/2a}$  of  $-4.0 \pm 3.1$  mV compared to no ranolazine controls ( $n=5$ ,  $P<0.05$ , two-sample t-test). These data from native myocytes support pressure sensitivity of  $\text{Na}_v1.5$  and inhibition of mechanosensitivity by ranolazine.



### Ranolazine reduces pressure-induced increase in the $\text{Na}_v1.5$ window current

Steady-state *window* is the area underneath the overlapping feet of activation and inactivation voltage dependence curves, where an appreciable portion of  $\text{Na}_v1.5$  channels is active (**Figure 2C, D**). We assessed pressure-dependent changes in window current activity using single channel recording. Cell-attached patches were stepped through a voltage ladder to determine the foot of activation. For the patch in **Figure 4A** this was  $-40$  mV and averaged  $-45 \pm 2.2$  mV ( $n=5$ ). For each patch, we set the holding potential (HP) to the foot of activation and recorded 300 pulses of 300 msec at the left edge of the window. We applied pressure for 100 msec (bracket) every 200 msec. Single channel openings were idealized over 50 msec intervals before (black bar) and during the  $-30$  mmHg pressure step (grey bar). On average, the number of single channel open events increased from  $85 \pm 40$  at rest to  $137 \pm 45$  with a  $-30$  mmHg pressure, representing a pairwise fractional increase ( $n=n_{30}/n_0$ ) with pressure of  $240 \pm 64\%$  ( $n=5$ ,  $P < 0.05$ ) (**Figure 4Ai**). Open channel lifetime did not change from  $0.50 \pm 0.11$  msec (control) to  $0.54 \pm 0.13$  msec (pressure), or a pairwise change ( $\tau = \tau_{30}/\tau_0$ ) by  $28 \pm 29\%$  ( $n=5$ ,  $P > 0.05$ ) (**Figure 4Aii**). Since the single channel conductance does not change with pressure<sup>11</sup>, the significant increase in the number of open channel events produced a steady-state  $\text{Na}^+$  charge  $Q_{30}/Q_0$  ( $[n_{30} * \tau_{30}] / [n_0 * \tau_0]$ ) increase of  $260 \pm 31\%$  ( $n=5$ ,  $P < 0.01$ , paired t-test). This significant increase in window current with pressure would depolarize the cell and likely make it more excitable.

Ranolazine ( $50 \mu\text{M}$ ) reduced the pressure-induced increase in window current activity (**Figure 4B**). At HP of  $40 \pm 6$  mV ( $n=3$ ), pressure failed to increase the number of single channel open events from  $134 \pm 29$  at rest to  $147 \pm 44$  with  $-30$  mmHg pressure, or pairwise change of  $9 \pm 14\%$  in the window open channel numbers ( $n=3$ ,  $P > 0.05$ ) (**Figure 4Bi**). Open channel lifetimes also did not change from  $0.66 \pm 0.10$  msec at rest to  $0.68 \pm 0.057$  msec, a pairwise change of  $4 \pm 6\%$  ( $n=3$ ,  $P > 0.05$ ) (**Figure 4Bii**). The result was no change in steady-state  $\text{Na}^+$  charge ( $14 \pm 20\%$ ,  $n=3$ ,  $P > 0.05$ ). These results suggest that pressure-induced increase in window current at resting potential is abolished by ranolazine.

### Ranolazine reduces pressure-induced increase in the $\text{Na}_v1.5$ late current open channel events

$\text{Na}^+$  late current is the small steady-state flux during the action potential plateau. Late current abnormalities have been implicated in cardiac pathologies such as LQT3<sup>27</sup>, ischemia<sup>28</sup> and heart failure<sup>15</sup>, and are thought to be the therapeutic target for ranolazine<sup>16</sup>. In a cell-attached configuration the late current is comprised of sporadic single channel events (**Figure 5A**). We used a 200 msec step depolarization from  $-100$  mV to  $0$  mV, and analyzed single channel events in the last 100 msec from individual patches at rest ( $0$  mmHg, data not shown) and then using a  $-30$  mmHg ramp pressure applied to the same patch (**Figure 5A**). Compared to the late single channel events at rest ( $19 \pm 5$ ),  $-30$  mmHg pressure produced an increase in event number ( $42 \pm 10$ ), or a  $235 \pm 44\%$  pairwise increase ( $n=4$ ,  $P < 0.05$ ) (**Figure 5Ai**). Single channel open lifetime trended to a decrease from control ( $0.61 \pm 0.11$  msec) to pressure ( $0.37 \pm 0.07$  msec), or a pairwise decrease by  $71 \pm 18\%$  ( $n=4$ ,  $P > 0.05$ ) (**Figure 5Aii**). Assuming no change in single channel conductance<sup>11</sup>, total late steady-state  $\text{Na}^+$  charge did not change ( $19 \pm 70\%$ ,  $n=4$ ,  $P > 0.05$ ). Ranolazine ( $50 \mu\text{M}$ ) abolished the pressure-induced changes in late current (**Figure 5B**). The single channel event number did not change from rest ( $40 \pm 14$ ) to negative pressure ( $28 \pm 5$ ), or a pairwise change of  $22 \pm 30\%$  ( $n=5$ ,  $P > 0.05$ ) (**Figure 5Bi**). Pressure also did not change open channel lifetime from  $0.52 \pm 0.10$  msec at  $0$  mmHg to  $0.61 \pm 0.02$  msec at  $-30$  mmHg, or a pairwise change of  $27 \pm 23\%$  ( $n=5$ ,  $P > 0.05$ ) (**Figure 5Bii**). Total late steady-state  $\text{Na}^+$  charge was not changed ( $34 \pm 79\%$ ,  $n=5$ ,  $P > 0.05$ ). Thus, the pressure-induced increase in late single channel opening numbers is abolished with ranolazine.

### F1760A mutation decreases Na<sub>v</sub>1.5 peak current block by ranolazine, but does not eliminate mechanoinhibition

Ranolazine block of Na<sub>v</sub>1.5 requires the putative local anesthetic binding site on DIVS6 F1760<sup>29</sup>. Hence, we investigated whether inhibition of mechanosensitivity by ranolazine could be altered by site-directed mutagenesis of residue F1760. In whole-cell voltage clamped HEK, F1760A Na<sub>v</sub>1.5 peak currents were insensitive to 50 μM ranolazine, as current densities changed only 2±6%, from -195±29 pA/pF in control to -201±32 pA/pF with drug (n=6, *P*>0.05) (**Figure 6**). Nevertheless, F1760A Na<sub>v</sub>1.5 channels appeared to retain mechanosensitivity like wild-type Na<sub>v</sub>1.5, as F1760A currents increased 18±5% from -195±29 pA/pF to -228±32 pA/pF in response to flow of drug-free solution (n=6, *P*<0.05). Moreover, inhibition of flow response was also retained in F1760A channels like wild-type; F1760A peak Na<sup>+</sup> currents were not inducible by flow of ranolazine solution, changing only 8±4% from -201±32 pA/pF with flow off to -213±30 pA/pF with flow on (n=6, *P*>0.05).

We confirmed these findings in cell-attached patches. At rest (0 mmHg), while the application of ranolazine decreased wild-type Na<sub>v</sub>1.5 current by 32±8% (n=4), the peak currents of F1760A Na<sub>v</sub>1.5 channels in presence of 50 μM ranolazine were decreased by only 11±9% (n=4, *P*<0.05 compared to wild type current) (**Figure 7A**). The F1760A Na<sub>v</sub>1.5 channels were mechanosensitive to a similar extent as the wild-type channels, with a -30 mmHg pulse producing Δ*V*<sub>1/2a</sub> of -10.8±2.5 mV (n=4), which was significantly reduced by 50 μM ranolazine to Δ*V*<sub>1/2a</sub> -4.7±1.8 mV (n=7) (*P*<0.05) (**Figure 7B**).

The above whole cell and cell-attached patch data confirm that F1760 is required for significant ranolazine block of Na<sub>v</sub>1.5 current at rest<sup>29</sup>. Yet, F1760A Na<sub>v</sub>1.5 retains mechanosensitivity, and ranolazine continues to inhibit F1760A Na<sub>v</sub>1.5 mechanosensitivity to a similar extent as in the wild-type Na<sub>v</sub>1.5. These results suggest that the ranolazine inhibition of Na<sub>v</sub>1.5 mechanosensitivity is not due to binding to F1760.

### Ranolazine inhibition of mechanosensitivity of Na<sub>v</sub>1.5 may require drug partitioning into the lipid bilayer

Ranolazine has a p*K*<sub>a</sub> of 7.17, so at pH 5 the positively charged form of ranolazine is roughly 100-fold more concentrated than the neutral form. We used pH 5 and 50 μM ranolazine in the pipette only for these experiments as bath acidity is known to affect multiple cellular processes. For a -30 mmHg pressure, wild-type Na<sub>v</sub>1.5 channels shifted the half-point of voltage sensitivity of activation Δ*V*<sub>1/2a</sub> by -7.4±1.0 mV (n=7) at pH 5 and -10.1±1.5 mV (n=5) at pH 7 (*P*>0.05). With the pipette containing 50 μM ranolazine and pH 5 solution, pressure produced a shift of Δ*V*<sub>1/2a</sub> of -5.2±1.7 mV (n=7), compared to -7.4±1.0 mV (n=7) without ranolazine (*P*>0.05) (**Figure 8A**). Thus, it appears that ionized ranolazine does not inhibit the shift in Δ*V*<sub>1/2a</sub> at pH 5. Since the ionized form of ranolazine does not significantly partition into the hydrophobic core of the bilayer, these data suggest that ranolazine inhibition of Na<sub>v</sub>1.5 mechanosensitivity may require bilayer partitioning.

The similarities of ranolazine and local anesthetics with respect to the overlapping binding sites and chemical properties (structure, log*P*, p*K*<sub>a</sub>) suggested that the mechanisms of action may also overlap. It is known that local anesthetics that exist in neutral forms, such as lidocaine, partition significantly into the hydrophobic core of the bilayer. Cell-attached patches were exposed to 50 μM lidocaine by addition to the bath as before. Lidocaine (50 μM) also blocked mechanosensitivity of Na<sub>v</sub>1.5, with pressure-induced Δ*V*<sub>1/2a</sub> -5.6±1.6 mV (n=5) (**Figure 8B**). This Δ*V*<sub>1/2a</sub> is smaller than -10.1±1.5 mV shift for the controls without lidocaine (**Figure 8A**). Thus, it appears that Na<sub>v</sub>1.5 mechanosensitivity block is not specific for ranolazine. We next used the permanently charged lidocaine homolog QX-314 to determine the need for bilayer partitioning for mechanosensitivity block. QX-314 is

membrane impermeable therefore we added 500  $\mu\text{M}$  QX-314 to the pipette solution. In the presence of QX-314,  $\text{Na}_V1.5$  mechanosensitivity persisted with a  $\Delta V_{1/2a}$   $-12.0 \pm 2.9$  mV ( $n=3$ ,  $P>0.05$  compared to lidocaine) (**Figure 8B**).

## Discussion

In this study we demonstrate  $\text{Na}_V$  mechanosensitivity in adult murine ventricular cardiac myocytes and in HEK cells transfected with  $\text{Na}_V1.5$ . We describe multiple effects of mechanical stimulation on  $\text{Na}_V1.5$  function and demonstrate effective inhibition of  $\text{Na}_V1.5$  mechanosensitivity by ranolazine and lidocaine. Furthermore, we establish that the inhibition of  $\text{Na}_V1.5$  mechanosensitivity by ranolazine does not require the established binding site, but appears to require bilayer partitioning.

Mechanical stimulation in cardiac myocytes and  $\text{Na}_V1.5$ -transfected HEK cells increased peak  $\text{Na}_V$  current, accelerated kinetics of activation and inactivation and in patches hyperpolarized the half-points of voltage-dependence of activation ( $V_{1/2a}$ ) and inactivation ( $V_{1/2i}$ ), thereby left-shifting the window current (**Figure 1, Figure 2A-C**). At the single channel level mechanical stimulation of  $\text{Na}_V1.5$  increased total window current at hyperpolarized resting potentials (**Figure 4A**) but not late current during depolarization to 0 mV (**Figure 5A**). These results suggest that  $\text{Na}_V1.5$  may contribute to MEF. In a cardiac myocyte membrane depolarization is the most consistent effect of stretch<sup>30</sup>. We showed two mechano-induced effects that would contribute to membrane depolarization: hyperpolarization of the  $\text{Na}_V1.5$  window current and a large increase in total  $\text{Na}^+$  charge density for small depolarizations (**Figure 2B, C**). On the other hand, for large depolarizations mechano-induced acceleration in inactivation led to a relative decrease in  $\text{Na}^+$  influx following the upstroke (**Figure 2B**). This may contribute to the early shortening of the action potential duration (APD) by stretch as previously shown<sup>31</sup>. However, stretch prolongs latter portions of APD<sup>30</sup>, which may predispose to development of secondary depolarization<sup>5</sup>. Stretch accelerates  $\text{Na}_V1.5$  inactivation and does not alter late current, so it is unlikely that  $\text{Na}_V1.5$  is involved in stretch-dependent ADP prolongation. Potential mechanisms include inhibition of  $\text{K}^+$  selective<sup>32</sup> or non-selective SACs<sup>33</sup>. In contrast, mechano-induced acceleration of  $\text{Na}_V1.5$  inactivation kinetics may protect from excessive stretch-dependent action potential prolongation. A recent study of the classic LQT3  $\text{Na}_V1.5$  mutations that have defective inactivation showed that pressure failed to accelerate inactivation in proportion to activation<sup>34</sup>, suggesting that pressure-induced acceleration of  $\text{Na}_V1.5$  inactivation may be a protective MEF response.

Ranolazine inhibited  $\text{Na}_V1.5$  mechanosensitivity in both cardiac myocytes and HEK cells. The drug diminished the mechano-induced increase in peak current, shift in voltage sensitivity (**Figure 1, Figure 2D-F**), increases in the window current (**Figure 4B**) and late current open channel event numbers (**Figure 5B**). Ranolazine inhibition of  $\text{Na}_V1.5$  mechanosensitivity would indicate multiple effects on stretch-dependence in a cardiac myocyte. Most obvious is that loss of the hyperpolarizing shift in voltage-dependence of activation and window current would decrease the excitability with stretch. Block of stretch-dependence of  $\text{Na}_V1.5$  inactivation would be more complex. We confirm that ranolazine left-shifts  $V_{1/2i}$  at rest<sup>35</sup> (**Supplemental Figure 3**) but we also show that it inhibits the mechano-induced leftward  $V_{1/2i}$  shift (**Supplemental Figure 4A**). Since  $V_{1/2i}$  shift is dose-dependent with respect to stretch<sup>11</sup>, the final result of  $V_{1/2i}$  position depends on doses of stretch and drug and would be difficult to predict.

The  $\text{IC}_{50}$  of ranolazine block of  $\Delta V_{1/2a}$ , the most sensitive pressure-sensitive parameter, was 54  $\mu\text{M}$  (**Figure 3**). This value is about five-fold higher than the accepted plasma concentration<sup>36</sup>. However, there are at least two reasons not to dismiss the inhibitory effect



of ranolazine on mechanosensitivity of Na<sub>v</sub>1.5. First, we do not know the true mechanical environment of the channels in situ. Previous data suggest that Na<sub>v</sub>1.5 mechanosensitivity is likely mediated by a combination of the lipid bilayer<sup>20</sup> and the cytoskeleton<sup>26</sup>. In the native setting, Na<sub>v</sub>1.5 resides within and associates with other mechano-relevant elements. Na<sub>v</sub>1.5 channels are localized within T-tubules<sup>37</sup> and caveolin-3 rich rafts<sup>38</sup>, which are membrane structures with high intrinsic curvature, and tend to be areas of mechanosensitivity<sup>39</sup>. The Na<sub>v</sub>1.5 channels also make extensive intracellular connections<sup>40</sup>. Some of the Na<sub>v</sub>1.5 associating proteins, such as ankyrin<sup>41</sup>, syntrophin<sup>42, 43</sup> and telethonin<sup>44</sup>, are known to be proteins involved in cellular mechanosensitivity. Dysfunctional interaction of Na<sub>v</sub>1.5 with associating proteins is known to contribute to pathology<sup>43, 45</sup>, so these connections may serve to further focus mechanical force at the channel<sup>45</sup>. While we used a -30 mmHg stimulus, which is at the lower end of the typical pressures used to study SACs<sup>6</sup>, the degree of mechanical stimulation in situ remains to be determined. Second, the membrane concentration of the drug likely differs from the plasma concentration. The neutral form of ranolazine is the effective inhibitor of Na<sub>v</sub>1.5 mechanosensitivity and it partitions substantially into the bilayer hydrophobic core. Membrane diffusion<sup>46</sup> and partition coefficients<sup>47</sup> increase with the extra energy, whether in the form of stretch or temperature. As our experiments were carried out at room temperature we expect that effective membrane concentration will further increase at physiologic temperature.

Our results shed some light on the mechanism of Na<sub>v</sub>1.5 mechanosensitivity. Inhibition by ranolazine does not require the putative binding site on DIVS6 (**Figure 7**) and neutral lidocaine and ranolazine inhibit, but charged ranolazine and permanently charged lidocaine analog QX-314 do not impact mechanosensitivity (**Figure 8**). This suggests the importance of drug partitioning into the lipid bilayer, but does not rule out other protein binding sites or cytoskeletal involvement. Previous studies support the importance of the lipid-protein interface in Na<sub>v</sub> function<sup>20</sup> and voltage-gated channel mechanosensitivity<sup>21</sup>. Many outstanding questions remain regarding the mechanism of Na<sub>v</sub>1.5 mechanosensitivity, but it very likely requires a combination of the associating proteins, membrane domains and protein-lipid interface.

This study demonstrates the mechanosensitivity of Na<sub>v</sub>1.5 in both native cardiac myocytes and a heterologous system. We establish drugs such as ranolazine, lidocaine and their analogs as pharmacologic tools for inhibition of Na<sub>v</sub>1.5 mechanosensitivity and suggest potential mechanisms. Further exploration of these compounds in disorders associated with MEF may be warranted. Examples include novel heart failure therapy<sup>48</sup> and atrial fibrillation related to stretch of pulmonary veins, recently shown to be suppressed by ranolazine<sup>49</sup>.

## Supplementary Material

Refer to Web version on PubMed Central for supplementary material.

## Acknowledgments

The authors would like to thank Dr. James Rae for valuable discussions and opinions on the manuscript.

**Funding Sources:** This work was supported by NIDDK 52766 and P30DK84567.

## References

1. Cooper PJ, Lei M, Cheng LX, Kohl P. Selected contribution: Axial stretch increases spontaneous pacemaker activity in rabbit isolated sinoatrial node cells. *J Appl Physiol.* 2000; 89:2099–2104. [PubMed: 11053369]

2. Lerman BB, Burkhoff D, Yue DT, Franz MR, Sagawa K. Mechanoelectrical feedback: Independent role of preload and contractility in modulation of canine ventricular excitability. *J Clin Invest.* 1985; 76:1843–1850. [PubMed: 4056056]
3. Sung D, Mills RW, Schettler J, Narayan SM, Omens JH, McCulloch AD. Ventricular filling slows epicardial conduction and increases action potential duration in an optical mapping study of the isolated rabbit heart. *J Cardiovasc Electrophysiol.* 2003; 14:739–749. [PubMed: 12930255]
4. Maron BJ, Poliac LC, Kaplan JA, Mueller FO. Blunt impact to the chest leading to sudden death from cardiac arrest during sports activities. *N Engl J Med.* 1995; 333:337–342. [PubMed: 7609749]
5. Wang Z, Taylor LK, Denney WD, Hansen DE. Initiation of ventricular extrasystoles by myocardial stretch in chronically dilated and failing canine left ventricle. *Circulation.* 1994; 90:2022–2031. [PubMed: 7522991]
6. Hu H, Sachs F. Stretch-activated ion channels in the heart. *J Mol Cell Cardiol.* 1997; 29:1511–1523. [PubMed: 9220338]
7. Morris CE. Voltage-gated channel mechanosensitivity: Fact or friction? *Frontiers in Physiology.* 2011;2. [PubMed: 21423412]
8. Gellens ME, George AL Jr, Chen LQ, Chahine M, Horn R, Barchi RL, Kallen RG. Primary structure and functional expression of the human cardiac tetrodotoxin-insensitive voltage-dependent sodium channel. *Proc Natl Acad Sci U S A.* 1992; 89:554–558. [PubMed: 1309946]
9. Li GR, Baumgarten CM. Modulation of cardiac  $\text{Na}^+$  current by gadolinium, a blocker of stretch-induced arrhythmias. *Am J Physiol Heart Circ Physiol.* 2001; 280:H272–279. [PubMed: 11123242]
10. Redaelli E, Cassulini RR, Silva DF, Clement H, Schiavon E, Zamudio FZ, Odell G, Arcangeli A, Clare JJ, Alagon A, de la Vega RC, Possani LD, Wanke E. Target promiscuity and heterogeneous effects of tarantula venom peptides affecting  $\text{Na}^+$  and  $\text{K}^+$  ion channels. *J Biol Chem.* 2010; 285:4130–4142. [PubMed: 19955179]
11. Beyder A, Rae JL, Bernard C, Strege PR, Sachs F, Farrugia G. Mechanosensitivity of  $\text{Nav}1.5$ , a voltage-sensitive sodium channel. *J Physiol.* 2010; 588:4969–4985. [PubMed: 21041530]
12. Morris CE, Juranka PF. Nav channel mechanosensitivity: Activation and inactivation accelerate reversibly with stretch. *Biophys J.* 2007; 93:822–833. [PubMed: 17496023]
13. Strege PR, Ou Y, Sha L, Rich A, Gibbons SJ, Szurszewski JH, Sarr MG, Farrugia G. Sodium current in human intestinal interstitial cells of cajal. *Am J Physiol Gastrointest Liver Physiol.* 2003; 285:G1111–1121. [PubMed: 12893628]
14. Burashnikov A, Di Diego JM, Zygmunt AC, Belardinelli L, Antzelevitch C. Atrium-selective sodium channel block as a strategy for suppression of atrial fibrillation: Differences in sodium channel inactivation between atria and ventricles and the role of ranolazine. *Circulation.* 2007; 116:1449–1457. [PubMed: 17785620]
15. Undrovinas AI, Belardinelli L, Undrovinas NA, Sabbah HN. Ranolazine improves abnormal repolarization and contraction in left ventricular myocytes of dogs with heart failure by inhibiting late sodium current. *J Cardiovasc Electrophysiol.* 2006; 17:S169–S177. [PubMed: 16686675]
16. Belardinelli L, Shryock JC, Fraser H. Inhibition of the late sodium current as a potential cardioprotective principle: Effects of the late sodium current inhibitor ranolazine. *Heart.* 2006; 92:iv6–iv14. [PubMed: 16775092]
17. Hille B. Local anesthetics: Hydrophilic and hydrophobic pathways for the drug-receptor reaction. *J Gen Physiol.* 1977; 69:497–515. [PubMed: 300786]
18. Lenkey N, Karoly R, Lukacs P, Vizi ES, Sunesen M, Fodor L, Mike A. Classification of drugs based on properties of sodium channel inhibition: A comparative automated patch-clamp study. *PLoS One.* 2010; 5:e15568. [PubMed: 21187965]
19. Undrovinas AI, Shander GS, Makielski JC. Cytoskeleton modulates gating of voltage-dependent sodium channel in heart. *Am J Physiol.* 1995; 269:H203–214. [PubMed: 7631850]
20. Lundbaek JA, Birn P, Hansen AJ, Sogaard R, Nielsen C, Girshman J, Bruno MJ, Tape SE, Egebjerg J, Greathouse DV, Mattice GL, Koeppe RE 2nd, Andersen OS. Regulation of sodium channel function by bilayer elasticity: The importance of hydrophobic coupling. Effects of micelle-forming amphiphiles and cholesterol. *J Gen Physiol.* 2004; 123:599–621. [PubMed: 15111647]

21. Schmidt D, Mackinnon R. Voltage-dependent k<sup>+</sup> channel gating and voltage sensor toxin sensitivity depend on the mechanical state of the lipid membrane. *Proc Natl Acad Sci U S A*. 2008; 105:19276–19281. [PubMed: 19050073]
22. Hodgson DM, Zingman LV, Kane GC, Perez-Terzic C, Bienengraeber M, Ozcan C, Gumina RJ, Pucar D, O'Coilain F, Mann DL, Alekseev AE, Terzic A. Cellular remodeling in heart failure disrupts k(atp) channel-dependent stress tolerance. *Embo J*. 2003; 22:1732–1742. [PubMed: 12682006]
23. Besch SR, Suchyna T, Sachs F. High-speed pressure clamp. *Pflugers Arch*. 2002; 445:161–166. [PubMed: 12397401]
24. Morris CE, Juranka PF, Lin W, Morris TJ, Laitko U. Studying the mechanosensitivity of voltage-gated channels using oocyte patches. *Methods Mol. Biol*. 2006; 322:315–329. [PubMed: 16739733]
25. Haufe V, Camacho JA, Dumaine R, Gunther B, Bollensdorff C, von Banchet GS, Benndorf K, Zimmer T. Expression pattern of neuronal and skeletal muscle voltage-gated na<sup>+</sup> channels in the developing mouse heart. *J Physiol*. 2005; 564:683–696. [PubMed: 15746173]
26. Stregre PR, Holm AN, Rich A, Miller SM, Ou Y, Sarr MG, Farrugia G. Cytoskeletal modulation of sodium current in human jejunal circular smooth muscle cells. *Am J Physiol Cell Physiol*. 2003; 284:C60–66. [PubMed: 12475760]
27. Bennett PB, Yazawa K, Makita N, George AL Jr. Molecular mechanism for an inherited cardiac arrhythmia. *Nature*. 1995; 376:683–685. [PubMed: 7651517]
28. Fraser H, Belardinelli L, Wang L, Light PE, McVeigh JJ, Clanachan AS. Ranolazine decreases diastolic calcium accumulation caused by atx-ii or ischemia in rat hearts. *J Mol Cell Cardiol*. 2006; 41:1031–1038. [PubMed: 17027025]
29. Fredj S, Sampson KJ, Liu H, Kass RS. Molecular basis of ranolazine block of I<sub>qt-3</sub> mutant sodium channels: Evidence for site of action. *Br J Pharmacol*. 2006; 148:16–24. [PubMed: 16520744]
30. Kamkin A, Kiseleva I, Isenberg G. Stretch-activated currents in ventricular myocytes: Amplitude and arrhythmogenic effects increase with hypertrophy. *Cardiovasc Res*. 2000; 48:409–420. [PubMed: 11090836]
31. Lab MJ. Mechanically dependent changes in action potentials recorded from the intact frog ventricle. *Circ Res*. 1978; 42:519–528. [PubMed: 630669]
32. Ji S, John SA, Lu Y, Weiss JN. Mechanosensitivity of the cardiac muscarinic potassium channel. A novel property conferred by kir3.4 subunit. *J Biol Chem*. 1998; 273:1324–1328. [PubMed: 9430664]
33. Ravens U. Mechano-electric feedback and arrhythmias. *Prog Biophys Mol Biol*. 2003; 82:255–266. [PubMed: 12732284]
34. Banderali U, Juranka PF, Clark RB, Giles WR, Morris CE. Impaired stretch modulation in potentially lethal cardiac sodium channel mutants. *Channels (Austin)*. 2010; 4:12–21. [PubMed: 20090423]
35. Rajamani S, El-Bizri N, Shryock JC, Makielski JC, Belardinelli L. Use-dependent block of cardiac late na<sup>(+)</sup> current by ranolazine. *Heart Rhythm*. 2009; 6:1625–1631. [PubMed: 19879541]
36. Jerling M. Clinical pharmacokinetics of ranolazine. *Clin Pharmacokinet*. 2006; 45:469–491. [PubMed: 16640453]
37. Cohen SA. Immunocytochemical localization of rh1 sodium channel in adult rat heart atria and ventricle. Presence in terminal intercalated disks. *Circulation*. 1996; 94:3083–3086. [PubMed: 8989112]
38. Vatta M, Ackerman MJ, Ye B, Makielski JC, Ughanze EE, Taylor EW, Tester DJ, Balijepalli RC, Foell JD, Li Z, Kamp TJ, Towbin JA. Mutant caveolin-3 induces persistent late sodium current and is associated with long-qt syndrome. *Circulation*. 2006; 114:2104–2112. [PubMed: 17060380]
39. Sinha B, Koster D, Ruez R, Gonnord P, Bastiani M, Abankwa D, Stan RV, Butler-Browne G, Vedio B, Johannes L, Morone N, Parton RG, Raposo G, Sens P, Lamaze C, Nassoy P. Cells respond to mechanical stress by rapid disassembly of caveolae. *Cell*. 2011; 144:402–413. [PubMed: 21295700]
40. Abriel H. Cardiac sodium channel na(v)1.5 and interacting proteins: Physiology and pathophysiology. *J Mol Cell Cardiol*. 2010; 48:2–11. [PubMed: 19744495]

41. Mohler PJ, Bennett V. Ankyrin-based cardiac arrhythmias: A new class of channelopathies due to loss of cellular targeting. *Curr Opin Cardiol.* 2005; 20:189–193. [PubMed: 15861006]
42. Ueda K, Valdivia C, Medeiros-Domingo A, Tester DJ, Vatta M, Farrugia G, Ackerman MJ, Makielski JC. Syntrophin mutation associated with long qt syndrome through activation of the nnos-sc5a macromolecular complex. *Proc Natl Acad Sci U S A.* 2008; 105:9355–9360. [PubMed: 18591664]
43. Ou Y, Strege P, Miller SM, Makielski J, Ackerman M, Gibbons SJ, Farrugia G. Syntrophin gamma 2 regulates scn5a gating by a pdz domain-mediated interaction. *J Biol Chem.* 2003; 278:1915–1923. [PubMed: 12429735]
44. Mazzone A, Strege PR, Tester DJ, Bernard CE, Faulkner G, De Giorgio R, Makielski JC, Stanghellini V, Gibbons SJ, Ackerman MJ, Farrugia G. A mutation in telethonin alters nav1.5 function. *J Biol Chem.* 2008; 283:16537–16544. [PubMed: 18408010]
45. Mohler PJ, Rivolta I, Napolitano C, LeMaillet G, Lambert S, Priori SG, Bennett V. Nav1.5 e1053k mutation causing brugada syndrome blocks binding to ankyrin-g and expression of nav1.5 on the surface of cardiomyocytes. *Proc Natl Acad Sci U S A.* 2004; 101:17533–17538. [PubMed: 15579534]
46. Oghalai JS, Zhao HB, Kutz JW, Brownell WE. Voltage- and tension-dependent lipid mobility in the outer hair cell plasma membrane. *Science.* 2000; 287:658–661. [PubMed: 10650000]
47. Sanchez V, Arthur GR, Strichartz GR. Fundamental properties of local anesthetics. I. The dependence of lidocaine's ionization and octanol:Buffer partitioning on solvent and temperature. *Anesth Analg.* 1987; 66:159–165. [PubMed: 3813059]
48. Chandler MP, Stanley WC, Morita H, Suzuki G, Roth BA, Blackburn B, Wolff A, Sabbah HN. Short-term treatment with ranolazine improves mechanical efficiency in dogs with chronic heart failure. *Circ Res.* 2002; 91:278–280. [PubMed: 12193459]
49. Sicouri S, Glass A, Belardinelli L, Antzelevitch C. Antiarrhythmic effects of ranolazine in canine pulmonary vein sleeve preparations. *Heart Rhythm.* 2008; 5:1019–1026. [PubMed: 18598958]

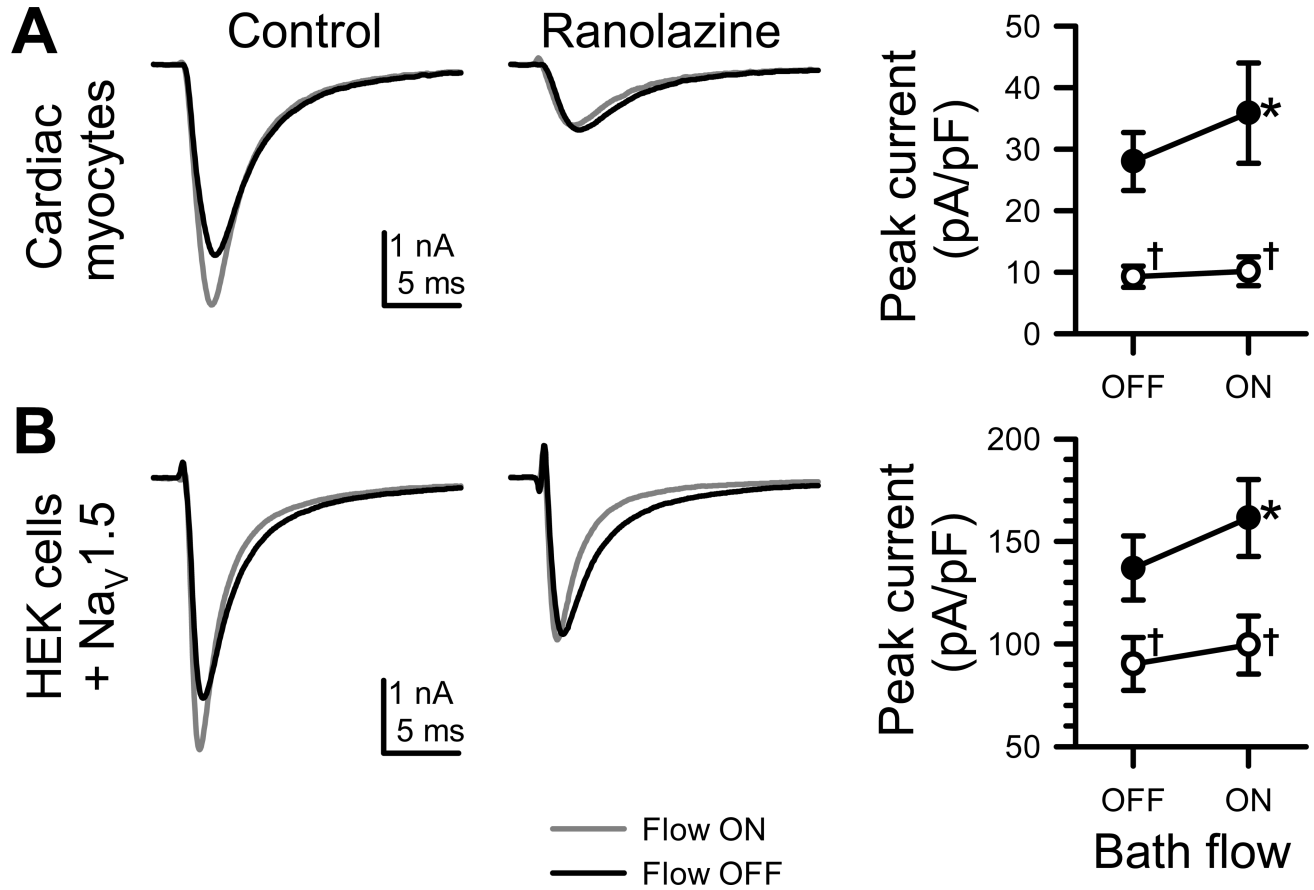


**Figure 1.** Ranolazine blocks mechanosensitive response and peak currents of Na<sup>+</sup> channels in murine cardiac myocytes and HEK cells transfected with Na<sub>v</sub>1.5. **Left, A**, Representative Na<sup>+</sup> currents recorded by whole cell voltage-clamp from murine cardiac myocytes and **B**, HEK cells transfected with Na<sub>v</sub>1.5, elicited by stepping to -30 mV from -120 mV before (*black traces, Flow OFF*) or during (*grey traces, Flow ON*) bath flow, produced by rinsing solution through the recording chamber at 10 mL/min in the absence (*Control, 0 μM*) or presence (*Ranolazine, 50 μM*) of drug. **Right**, Average peak current densities in response to flow of solution without (*filled symbols*) or with (*empty symbols*) ranolazine (n=5; \*P<0.05 compared to *Flow OFF*; †P<0.05 compared to 0 μM ranolazine, and P<0.05 interaction between flow and ranolazine blockade by two-way repeated measures ANOVA with Bonferroni multiple comparisons posttest).



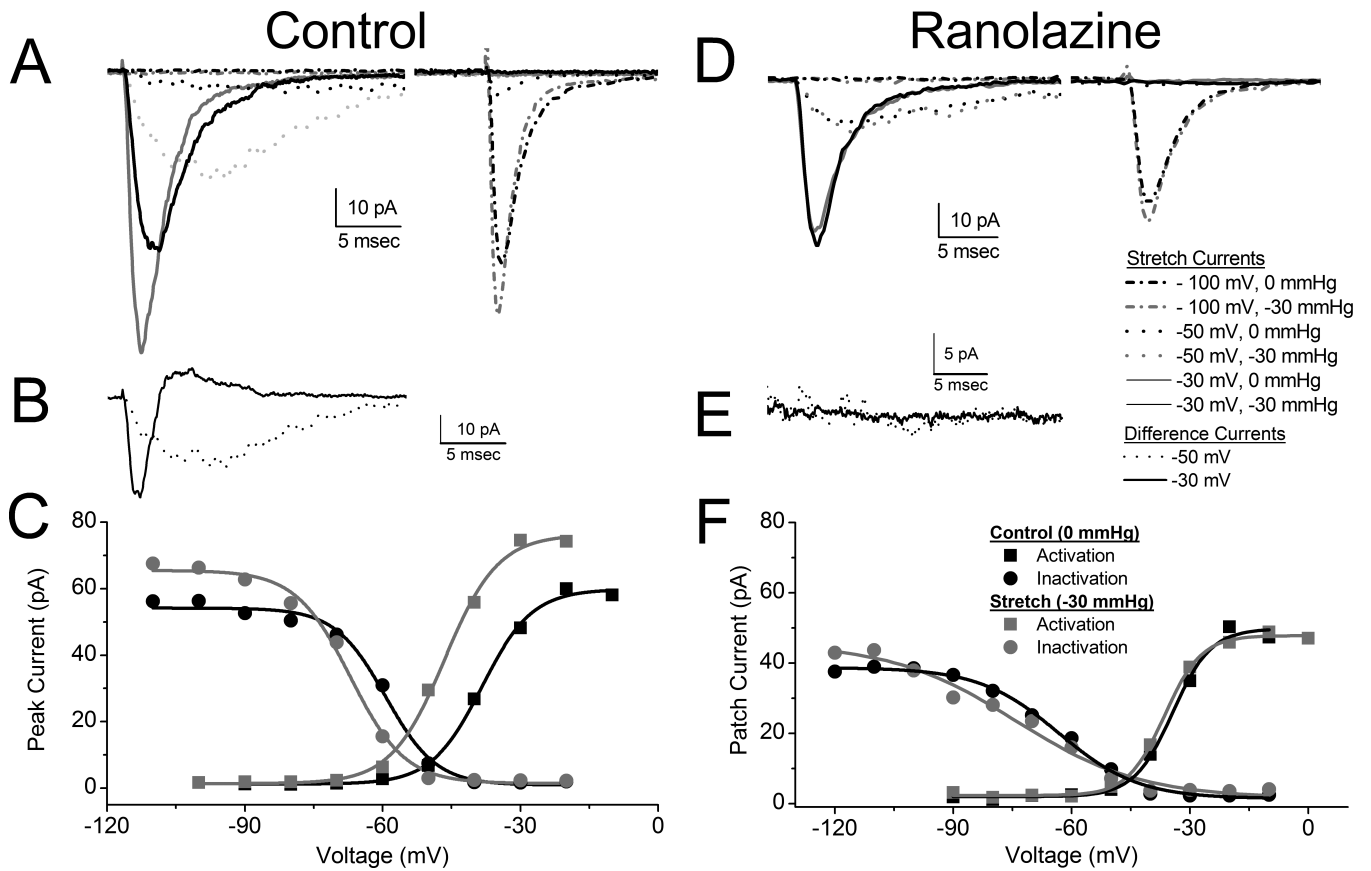


**Figure 2.**

Ranolazine blocks pressure-induced increase in peak current and hyperpolarizing shift of the voltage-dependence of activation and inactivation. **A, B, C** are controls and **D, E, F** are ranolazine (50  $\mu$ M). **A & D**, single patch average Na<sup>+</sup> currents elicited by stepping to -100 mV (dash dot) -50 mV (dot), -30 mV (solid) from -140 mV at 0 mmHg (black) and at -30 mmHg pressure (grey). First peak is activation and second peak is inactivation (availability). **B & E**, same patch difference currents ( $I_{-30} - I_0$ ) shown for -50 mV (dot black) and -30 mV (solid black). **C & F**, peak current-voltage (IV) for this patch at 0 mmHg (black) and -30 mmHg (grey), with activation (boxes) and inactivation (circles). Solid lines are Boltzmann fits of 0 mmHg (black) and -30 mmHg (grey).

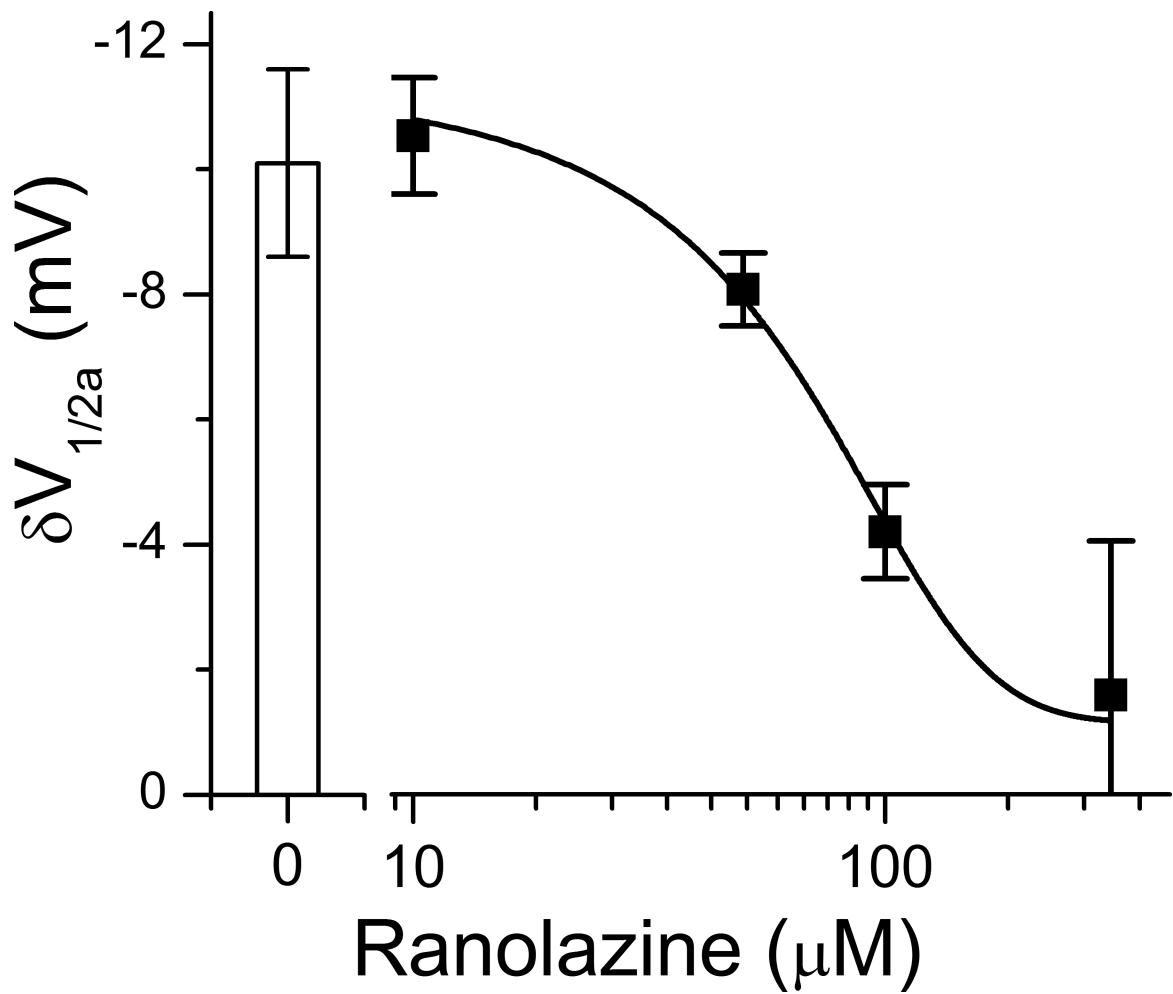


**Figure 3.** Ranolazine blocks mechanosensitivity of  $\text{Na}_v1.5$  in a concentration-dependent manner. Bar graph is shift in the voltage dependence of activation ( $\Delta V_{1/2a}$ ) for 0  $\mu\text{M}$  ranolazine and scatter plot is  $\Delta V_{1/2a}$  versus increasing ranolazine concentrations. Solid line is a dose-response fit with  $\text{IC}_{50}$  of 53.6  $\mu\text{M}$ .

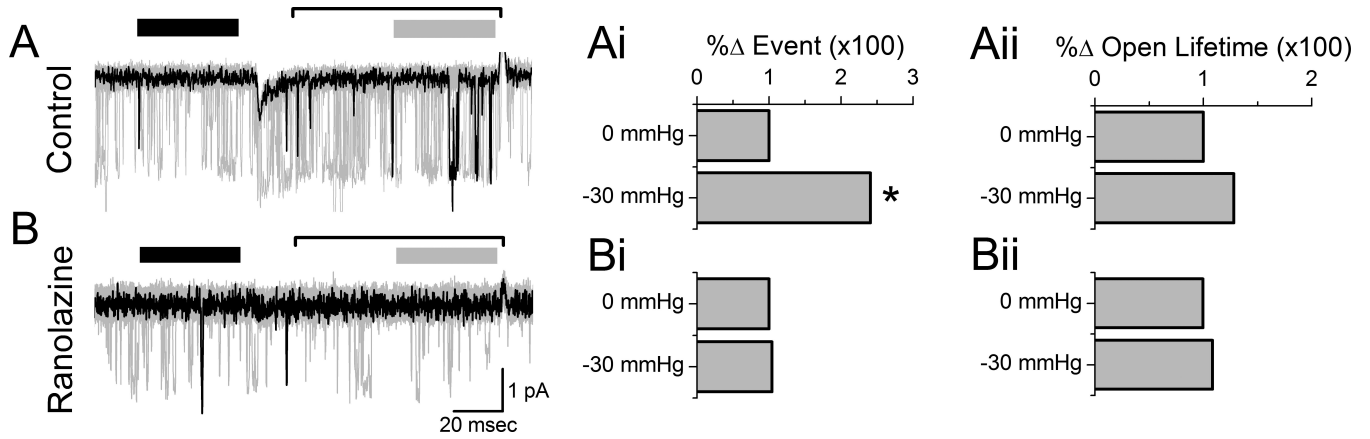


**Figure 4.**

Ranolazine inhibits pressure-induced increase in window current. **A** are controls and **B** are ranolazine (50  $\mu$ M). **A & B**, single channel Na<sup>+</sup> window current at HP -40 mV typical (black) and overlaid first fifty 300 msec traces (grey) at 0 mmHg and -30 mmHg (bracket). Single channel activity idealized before (black bar) and during (grey bar) the pressure pulse. Bar graphs show for -30 mmHg compared to 0 mmHg percent change of open channel event number ( $\#_{30}/\#_0 \times 100$ ) for control (**Ai**) and 50  $\mu$ M ranolazine (**Bi**), and open channel lifetime ( $\tau_{30}/\tau_0 \times 100$ ) for control (**Aii**) and 50  $\mu$ M ranolazine (**Bii**) (n=5, \* $P$ <0.05; paired t-test for events between 0 mmHg and -30mmHg).

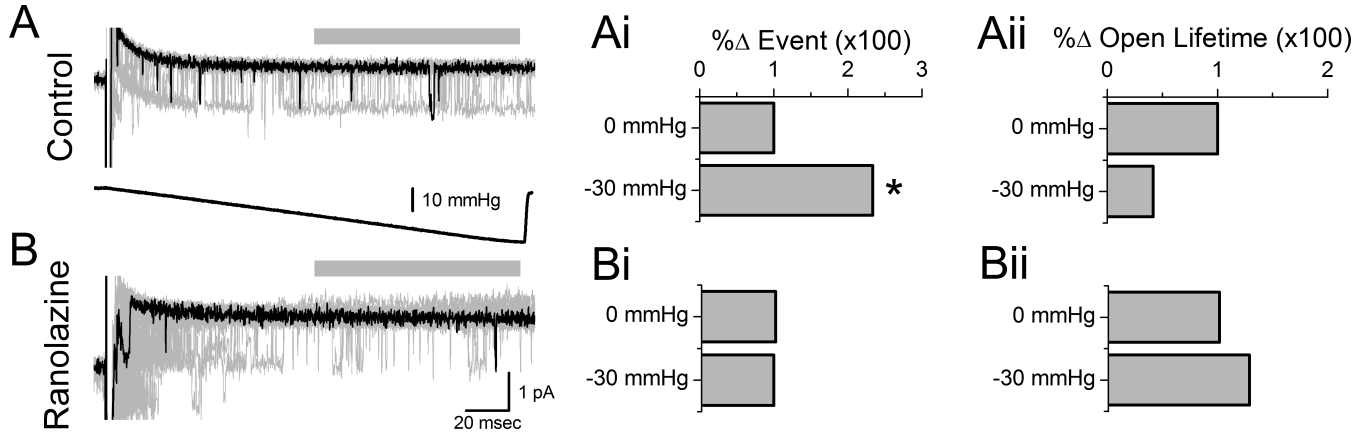


**Figure 5.** Ranolazine inhibits pressure-induced increase in late open channel event number. **A** are controls and **B** are ranolazine (50 μM). **A & B**, single channel Na<sup>+</sup> late current typical (black) and overlaid first fifty (grey) 200 msec long depolarizing pulses to 0 mV from HP -100 mV for ramp to -30 mmHg (bottom). Single channel activity in the last 100 msec of late current activity analyzed (grey bars). Bar graphs show for -30 mmHg compared to 0 mmHg percent change in open channel event number ( $\#_{30}/\#_0 \times 100$ ) for control (**Ai**) and 50 μM ranolazine (**Bi**), and for open channel lifetime ( $\tau_{30}/\tau_0 \times 100$ ) for control (**Aii**) and 50 μM ranolazine (**Bii**) (n=4, \* $P < 0.05$ ; paired t-test for events between 0 mmHg and -30mmHg).

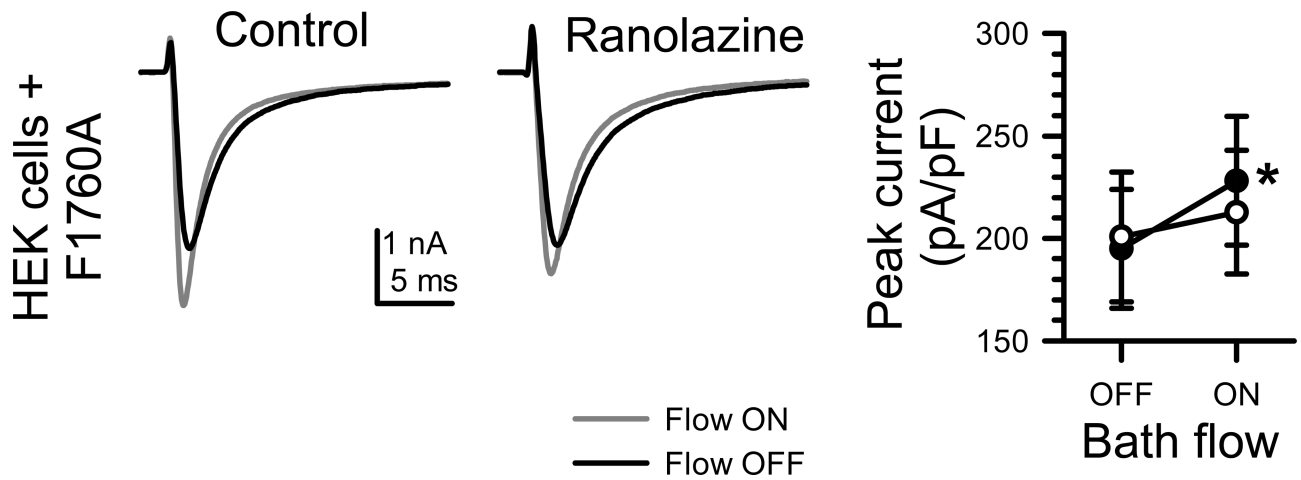


**Figure 6.**

Ranolazine blocks a mechanosensitive response but does not reduce peak currents of Na<sub>v</sub>1.5 F1760A expressed in HEK cells. *Left*, Na<sup>+</sup> currents elicited by stepping to -30 mV from -120 mV before (*black, Flow OFF*) or during (*grey, Flow ON*) bath flow, produced by rinsing solution through the recording chamber at 10 mL/min in the absence (*Control, 0 μM*) or presence (*Ranolazine, 50 μM*) of drug. *Right*, Average peak current densities of Na<sub>v</sub>1.5 F1760A in response to flow of solution without (*filled symbols*) or with (*empty symbols*) 50 μM ranolazine (n=6; \*P<0.05 compared to *Flow OFF*, P>0.05 compared to 0 μM ranolazine, and P>0.05 interaction between flow and ranolazine blockade by two-way repeated measures ANOVA with Bonferroni multiple comparisons posttest).



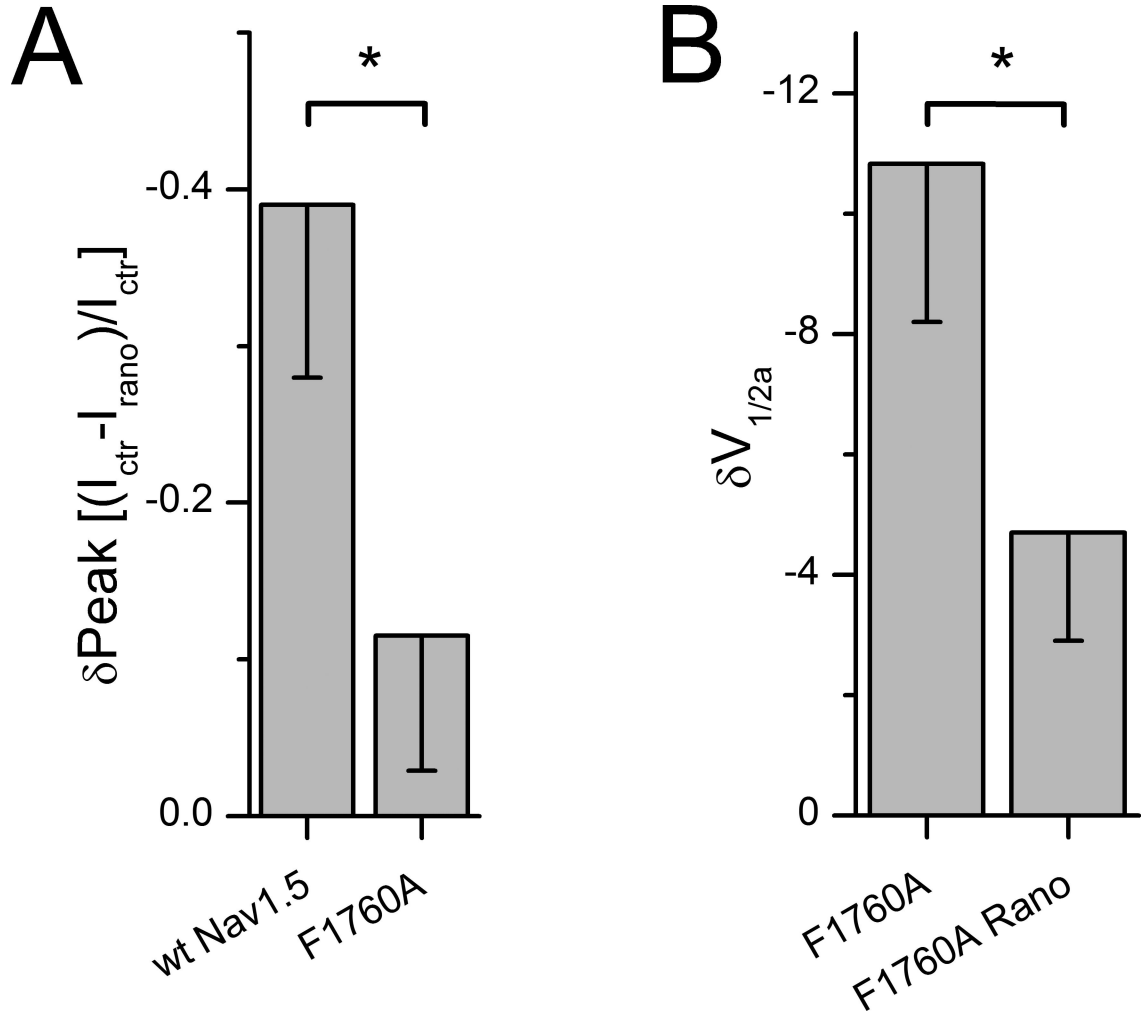


**Figure 7.**

Ranolazine block of mechanosensitivity is independent of F1760. **A**, the fractional decrease in peak current  $[(I_{\text{ctr}} - I_{\text{rano}}) / I_{\text{ctr}}]$  obtained from peak of IV curves in response to 50  $\mu\text{M}$  ranolazine for wild-type  $\text{Nav}1.5$  (*left*) and F1760A (*right*) ( $n=4$ ;  $*P<0.05$ ; two-sample t-test). **B**, mechanosensitivity of F1760A shown as a shift in half-point of voltage-dependence of activation ( $\Delta V_{1/2a}$ ) without ranolazine and significantly reduced with 50  $\mu\text{M}$  ranolazine ( $n=4-7$ ,  $*P<0.05$ ; two sample t-test).

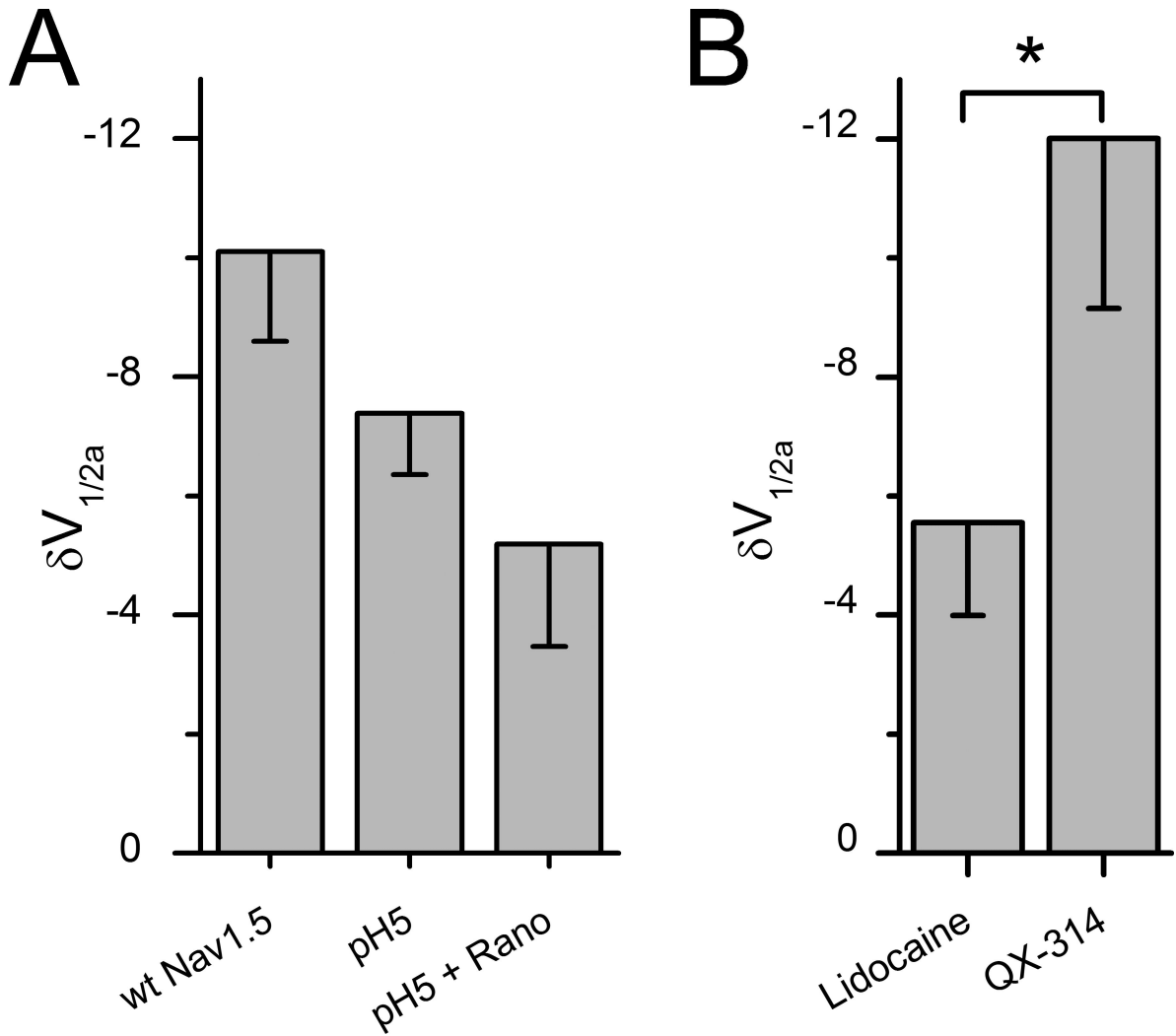


**Figure 8.**

Neutral ranolazine and lidocaine block mechanosensitivity of  $\text{Na}_V1.5$ . **A**, In cell-attached patches, pressure-induced  $\Delta V_{1/2a}$  with wt  $\text{Na}_V1.5$  in Ringer solution at pH 7.4 was not statistically different from  $\Delta V_{1/2a}$  when the pipette solution contained Ringer solution at pH 5 ( $n=5-7$ ,  $P>0.05$ ; two-sample t-test).  $\Delta V_{1/2a}$  was also not statistically different for pH 5 solution and ranolazine (50  $\mu\text{M}$ ) in pH 5 solution ( $n=7$ ,  $P>0.05$ ; two-sample t-test). **B**, Shift in  $V_{1/2a}$  with pressure with lidocaine (50  $\mu\text{M}$ ) is significantly less than with QX-314 (500  $\mu\text{M}$ ) ( $n=3-5$ ,  $*P<0.05$ ; two-sample t-test).